

Hydropower Aggregation by Spatial Decomposition – An SDDP Approach

Arild Helseth, Birger Mo

***Abstract*—The balance between detailed technical description, representation of uncertainty and computational complexity is central in long-term scheduling models applied to hydro-dominated power system. The aggregation of complex hydropower systems into equivalent energy representations (EER) is a commonly used technique to reduce dimensionality and computation time in scheduling models. This work presents a method for coordinating the EERs with their detailed hydropower system representation within a model based on stochastic dual dynamic programming (SDDP). SDDP is applied to an EER representation of the hydropower system, where feasibility cuts derived from optimization of the detailed hydropower are used to constrain the flexibility of the EERs. These cuts can be computed either before or during the execution of the SDDP algorithm and allow system details to be captured within the SDDP strategies without compromising the convergence rate and state-space dimensionality. Results in terms of computational performance and system operation are reported from a test system comprising realistic hydropower watercourses.**

***Index Terms*—Hydroelectric power generation, Power generation scheduling, Optimization methods, Stochastic Processes.**

NOMENCLATURE

A. Index Sets

$a \in \mathcal{A}$	Set of price areas;
$c \in \mathcal{C}^{B/F}$	Set of Benders (B) or feasibility (F) cuts;
$d \in \mathcal{D}_a$	Set of price-elastic demands;
$g \in \mathcal{G}_a$	Set of thermal units;
$h \in \mathcal{H}_a$	Set of hydropower modules;
$k \in \mathcal{K}$	Set of time steps within decision stage;
$\ell \in \mathcal{L}_a^{+/-}$	Set of lines directed to (+) or from (-) a;
$n \in \mathcal{N}_h$	Set of discharge segments;
$j \in \Omega_h^{S/C}$	Set of hydropower modules, defined Sec. III-A;
$j \in \omega_h^{D/B/S}$	Set of upstream modules discharging (D), bypassing (B) or spilling (S) to h.

B. Parameters

β_{ct}^B	Right-hand side for Benders cut, in €;
β_{act}^F	Right-hand side for feasibility cut, in GWh;
C_{dt}^D	Marginal value for demand, in €/GWh;
C_{gt}^G	Marginal cost for thermal gen., in €/GWh;
C^R	Marginal cost of curtailment, in €/GWh;
Δ_{ht}	Max. change in discharge, in m^3/s;
D_{atk}	Firm demand, in GWh;
$\mathbf{\Phi}$	Inflow correlation matrix;
ϕ_{at}	Fraction of controllable inflow to EER;
$\overline{F}_{\ell t}$	Max. capacity on line ℓ, in GWh;
ϵ_t	Inflow white noise;
η_{nh}	Efficiency at segment n, in $MW/m^3/s$;
η_h^b	Best efficiency point, in $MW/m^3/s$;
η_h^{bS}	Best eff. to sea, in $MW/m^3/s$;
η_h^{bC}	Best eff. for controllable inflow, in $MW/m^3/s$;
Γ_w	Conversion to Mm^3;
Γ_e	Conversion to GWh;
$\gamma^{p/v}, \kappa^{v/i}$	Coefficients for feasibility cut, fraction;
I_{at}	Energy inflow to EER, in GWh;
$\tilde{I}_{at}$	Average energy inflow to EER, in GWh;
I_{ht}	Inflow to module, in Mm^3;
$\tilde{I}_{ht}$	Average inflow, in Mm^3;
μ_{at}	Inflow mean value, in GWh;
NS	Number of scenarios s in SDDP forward it.;
π_{act}^v	Volume coeff. for Benders cut, in €/GWh;
$\boldsymbol{\pi}^z$	Vector of inflow coefficients for Benders cut;
$\overline{P}_{gt}^G$	Max. generation capacity, in GWh;
$\overline{P}_{dt}^D$	Max. price-elastic demand, in GWh;
$\underline{P}_{at}^H, \overline{P}_{at}^H$	Max./Min. EER generation, in GWh;
$\overline{P}_{ht}^H$	Max. generation capacity, in MW;
Ψ	End-of horizon valuation of water;
$\overline{Q}_{nht}^D$	Upper bound for discharge segment, in m^3/s;
σ_{at}	Inflow standard deviation, in GWh;
T	Number of decision stages t;
$\underline{V}_{at}, \overline{V}_{at}$	Max./Min. EER reservoir volume, in GWh;
$\underline{V}_{ht}, \overline{V}_{ht}$	Max./Min. reservoir volume, in Mm^3;
W_{atk}	Wind power, in GWh;
ζ_k	Fraction of weekly time covered by step k;
ζ_{aht}^V	Distribution factors for volume;
ζ_{aht}^I	Distribution factors inflow;
$\mathbf{z}_t$	Vector of normalized inflows z_{at}.

C. Decision Variables

α_t	Future expected cost, in €;
$f_{\ell tk}$	Flow on line ℓ, in GWh;
p_{gtk}^G	Generation from thermal unit, in GWh;
p_{dtk}^D	Price-elastic demand, in GWh;
p_{atk}^H	Hydropower generation per EER, in GWh;
p_{htk}^H	Hydropower generation per module, in MW;
q_{atk}^S	Spillage from EER reservoir, in GWh;
q_{htk}^D	Discharge through station, in m^3/s;
q_{nhtk}^D	Discharge through segment, in m^3/s;
q_{htk}^B	Bypass passing station, in m^3/s;
q_{htk}^S	Spillage from reservoir, in m^3/s;
r_{atk}	Curtailed power, in GWh;
$\mathbf{v}_t$	Vector of EER reservoir volumes v_{at}, in GWh;
v_{atk}	EER reservoir volume, in GWh;
v_{htk}	Reservoir volume, in Mm^3;
x_t, y_t	State and stage variables;
y_{tk}^P / y_t^E	Slack variables, in GWh.

I. INTRODUCTION

Long-term scheduling (LTS) of hydropower storages is an important task in hydro-dominated power systems which is typically accommodated in a single optimization model with a planning horizon of multiple years. LTS models support operational decision making through computation of strategies for hydropower utilization in terms of dual information (water values or prices) or volume targets. These strategies are applied in medium- and short-term models [1], and the coordination of such models can be organized in scheduling toolchains, as is the current practice in countries such as Brazil and Norway [2]. In addition, LTS models are used for planning tasks, such as system analyses [3], expansion planning [4], and maintenance planning [5]. While LTS models emphasize on the representation of uncertainties over the planning horizon typically using a rather coarse description of the technical system, shorter-term models are oriented towards deterministic formulations and a detailed physical system description [6], [7]. System simplifications in LTS models could lead to time-inconsistent policies [8], revealing a need for embedding more details from the short-term scheduling into LTS models [9]. However, as LTS models are typically not used for detailed system dispatch, one is primarily interested in the impact of the finer technical details rather than the detailed results.

A. Helseth and B. Mo are with SINTEF Energy Research, Trondheim, Norway (e-mail: arild.helseth@sintef.no)

This is the accepted version of an article published in IEEE Transactions of Sustainable Energy
https://doi.org/10.1109/TSTE.2022.3214497

A variety of methodologies have been proposed for solving the LTS problem, see e.g. the review by [10]. The use of methods based on optimization has matured over the last decades [11], and in particular the stochastic dual dynamic programming (SDDP) algorithm introduced in [12] has been widely applied in operative scheduling models [13]–[15], and is subject to improvements and extensions by the research community [16]–[22].

Although SDDP allows for efficient treatment of systems with multiple reservoirs, explicit treatment of physical reservoirs in large-scale systems may lead to prohibitive computation times, as demonstrated for the Norwegian system in [23]. A commonly used practice for reducing computational complexity is to aggregate the physical description of watercourses (or cascades) into an equivalent energy representation (EER) of the reservoirs and plants [13], [15], [24], [25]. The use of EERs, where the sum of potential energy in the reservoirs is represented rather than the water in each reservoir, was introduced in [26], and is often found to be a reasonable approximation for systems with large regulation capability and hydrologically homogenous basins [27]. As discussed in [28], and later demonstrated in [29], local constraints on reservoirs, flows and generations are not explicitly accounted for in such aggregated models, which may lead to suboptimal use of hydropower resources.

Various techniques have been applied to coordinate the representation of EERs and the detailed hydropower system within LTS models. In the EMPS model, which is widely applied for analyses of the Nordic power market, a detailed drawdown model based on heuristics is applied to dynamically improve the EER representation within a framework based on stochastic dynamic programming and system simulation [30], [31]. In the official Brazilian LTS model NEWAVE, the various EER attributes are estimated prior to running the SDDP model, as discussed in [25]. A method to consider hydraulically coupled systems in the construction of the EERs is presented in [32]. Moreover, a comparison between the use of EERs per subsystem and per cascade is provided in [33]. The NEWAVE model allows for a hybrid approach, where the individual reservoirs are considered in a first part of the planning horizon and then coupled to an EER representation covering the remaining horizon [15]. The hybrid approach is primarily useful when the LTS model is part of a toolchain leading to operational decisions.

Recent works apply genetic algorithms [34] and bilevel optimization [35], [36] to build hydropower equivalents for shorter-term and deterministic hydropower scheduling models. Despite promising results, these approaches do not easily fit into LTS model frameworks based on stochastic dynamic programming principles.

Based on the literature review above, there is clearly a need for LTS models and methodologies based on approximation of the detailed hydropower system, appropriately balancing the trade-off between accuracy of results and computational performance. Considering typical LTS application areas, modest computation times are important to facilitate many and frequently repeated analyses. In this context, we propose a method where the LTS problem is modeled by use of EERs to represent the hydropower, and SDDP is applied to solve the problem. It is demonstrated how each EER can interact with its underlying detailed hydropower description through linear inequalities (referred to as *feasibility cuts* in the following) added in the SDDP algorithm. Provided trial EER solutions, the feasibility cuts are derived by separately optimizing the detailed hydropower watercourses, and thus represent the system limitations through a spatial decomposition approach. The overall motivation is to increase the accuracy of hydropower representation in LTS models, while maintaining the convergence properties and low state space dimensionality obtained when representing complex hydropower systems by EERs.

Unlike previous works, the use of feasibility cuts provides a formal linkage between the aggregated and the detailed hydropower representation per EER within the SDDP algorithm. In contrast to the hybrid approach in [15], hydropower details are considered through the entire planning horizon seen by SDDP. The use of global feasibility cuts to deal with functionality that is not explicit in the SDDP formulation has previously been applied for embedding risk measures [37], [38] in LTS model formulations. Differently from those works, we use feasibility cuts to facilitate spatial decomposition, coordinating aggregated and detailed hydropower representations within the SDDP algorithm.

The main contributions from this work can be summarized as follows:

- A methodology for dynamically constraining the EER of hydropower within the SDDP algorithm by use of feasibility cuts per watercourse is presented. The feasibility cuts can be computed in the forward SDDP iterations and are shared among different states within each decision stage, and thus allows computationally efficient integration with the SDDP algorithm.
- The use of feasibility cuts computed prior to solving the SDDP model is described. Through a priori computation and removal of identical cuts it is demonstrated that computation time can be significantly reduced without compromising solution quality.

II. Problem Description

The LTS optimization problem is generally defined in (1), comprising state variables x_t and stage variables y_t for each decision stage t. One seeks to find an operating strategy that minimizes the expected cost of supplying electricity in (1a), accounting for the end-of-horizon valuation of stored water in $\Psi(x_T)$, and respecting constraints in (1b)-(1d). In this work a planning horizon of multiple years is applied, assuming weekly decision stages, allowing a finer time discretization within the week. Reservoir volumes and inflows for the EERs are considered as state variables. The stage variables represent the operational decisions to be made in each stage, while state variables transfer information about the system state between stages.

$$\min_{(x_1,y_1),\ldots,(x_T,y_T)} \mathbb{E}\left\{ \sum_{t=1}^{T} f_t(x_t, y_t) + \Psi(x_T) \right\} \tag{1a}$$

$$\text{s.t.} \quad \mathbf{W}x_t + \mathbf{H}x_{t-1} + \mathbf{G}y_t = h(\xi_t) \tag{1b}$$

$$\mathbf{B}y_t = 0 \tag{1c}$$

$$(x_t, y_t) \in X_t \tag{1d}$$

$$\forall t \in \{1, 2, \ldots, T\}$$

The constraints are indicated in (1b)-(1d), where the initial state vector x_0 is given, X_t is the feasible set for the decision variables of time step t, and $\mathbf{W}$, $\mathbf{H}$, $\mathbf{G}$, and $\mathbf{B}$, are matrices of suitable dimensions. The expectation in (1a) is taken over the stochastic inflow. Inflow to the EERs is represented by a vector autoregressive model of first order according to the procedure described in [39]. The right-hand-side parameter vector $h(\xi_t)$ in (1b) is dependent on the random vector of inflow "white noise" ξ_t whose distribution is known, and where ξ_t are the realizations.

The problem in (1) can be classified as a multi-stage stochastic optimization problem, which may be efficiently solved by decomposition techniques [40]. In the following we will use the SDDP algorithm, which is a sampling-based variant of multi-stage Benders decomposition. The problem in (1) can be decomposed into stage-wise nested linear programming (LP) problems of type:

This is the accepted version of an article published in IEEE Transactions of Sustainable Energy
https://doi.org/10.1109/TSTE.2022.3214497

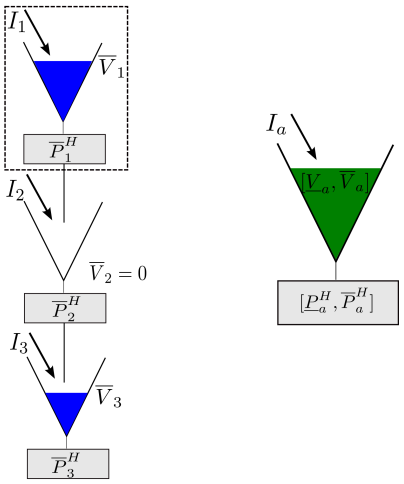

Fig. 1: Aggregation of a hydropower watercourse (left) to an EER (right).

$$\mathcal{Q}_t(x_{t-1}) = \min_{x_t, y_t} f_t(x_t, y_t) + \alpha_t(x_t) \tag{2a}$$

$$\text{s.t.} \quad (x_t, y_t) \in X_t(x_{t-1}, \xi_t) \tag{2b}$$

The variable α_t expresses the future expected cost function seen from the end of stage t. This variable will gradually be constrained by Benders cuts constructed in the SDDP iterations, as will be explained in detail later.

In Section III we elaborate on the stage-wise decision problem in (2), while the solution strategy for solving (1) is outlined in Section IV.

III. Stage-wise Decision Problem

In this section the stage-wise decision problem in (2) is described in detail. It is assumed that the hydropower is aggregated in EERs and that each EER represents a single watercourse and belongs to a separate price area (or bidding zone). These assumptions are without loss of generality, as the formulations could be adapted so that an EER represents multiple watercourses and with multiple EERs within a price area. Further division of multiple EERs per watercourse, as discussed in [32], is not possible without modeling adjustments.

A. Hydropower System Aggregation

The procedure for aggregating a watercourse to an EER is illustrated in Fig. 1 and described below. A watercourse comprises connected hydropower modules, each with a reservoir and a power station, as illustrated within the stapled rectangle to the upper left in Fig. 1. Inflow is directed into the reservoirs, and both reservoirs and power stations may have zero capacity in a module, such as the dummy reservoir with zero storage capacity in module 2 in Fig. 1.

Hydropower generation for a power station is represented as a piecewise linear and concave relationship between power and discharge, represented by a set of discharge segments with decreasing efficiency, as illustrated in Fig. 2. A power station typically comprises multiple generation units, and [41] provides a description on how power station production functions can be derived through data per generation unit. Each hydropower station has a best efficiency point η_h^b which represents the efficiency of the first segment.

A best efficiency point referred to sea level can be defined as in (3a), where Ω_h^S comprises the modules from module h and downstream. Converting inflow for a reservoir h to EER energy inflow involves a separation between controllable and non-controllable water. For each module we define best efficiency referred sea level for the controllable part of the inflow in (3b), where Ω_h^C comprises the modules from module h and downstream starting at the first reservoir with non-zero storage capacity. From the example in Fig. 1, $\Omega_1^S = \Omega_1^C = \{1, 2, 3\}$, $\Omega_2^S = \{2, 3\}$, $\Omega_2^C = \{3\}$, $\Omega_3^S = \Omega_3^C = \{3\}$.

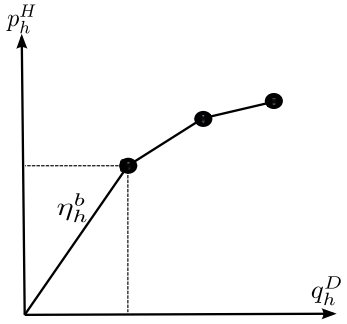

Fig. 2: Relationship between power and discharge for a hydropower module.

$$\eta_h^{bS} = \sum_{j \in \Omega_h^S} \eta_h^b \tag{3a}$$

$$\eta_h^{bC} = \sum_{j \in \Omega_h^C} \eta_h^b \tag{3b}$$

The properties of the EER per decision stage t are defined in (4). These parameters are calculated in advance and kept constant when optimizing the system by use of SDDP. Average energy inflow is found in (4a), and the controllable fraction of the energy inflow is defined in (4b). Maximum and minimum storage capacities are found in (4d) and (4c), respectively. The maximum generation capacity of the EER is found as the sum of the individual capacities in (4f), while the minimum generation depends on non-controllable inflow in (4e).

$$\tilde{I}_{at} = \sum_{h \in \mathcal{H}_a} \Gamma_e \eta_h^{bS} \tilde{I}_{ht} \tag{4a}$$

$$\phi_{at} = \frac{\sum_{h \in \mathcal{H}_a} \Gamma_e \eta_h^{bC} \tilde{I}_{ht}}{I_{at}} \tag{4b}$$

$$\underline{V}_{at} = \sum_{h \in \mathcal{H}_a} \Gamma_e \eta_h^{bS} \underline{V}_{ht} \tag{4c}$$

$$\overline{V}_{at} = \sum_{h \in \mathcal{H}_a} \Gamma_e \eta_h^{bS} \overline{V}_{ht} \tag{4d}$$

$$\underline{P}_{at}^H = (1 - \phi_{at}) \cdot \tilde{I}_{at} \tag{4e}$$

$$\overline{P}_{at}^H = \sum_{h \in \mathcal{H}_a} \Gamma_e \overline{P}_{ht}^H \tag{4f}$$

The aggregated hydropower description in (4) will, for most detailed system configurations, overestimate the flexibility of the hydropower system, since energy conversion refers to best efficiencies and EER capacities are found as the sum of module capacities. In Section III-C it is described how the flexibility of EERs can be constrained by linear inequalities found by optimizing operation of the detailed hydropower system. It should be noted that EER parameters can be derived differently, to incorporate features such as the dependency of energy conversion and maximum power generation on reservoir level, and losses in the non-controllable inflows due to spillage, see e.g. [25], [26], [32], [42]. In the presented approach, it is recommended to include such features in the detailed hydropower

This is the accepted version of an article published in IEEE Transactions of Sustainable Energy
https://doi.org/10.1109/TSTE.2022.3214497

model described in Section III-C to further constrain EER operation by feasibility cuts.

B. Decision Problem

The decision problem for a week t is defined as an LP problem in (5), detailing the general formulation in (2). The hydropower system is aggregated in EERs, and the vector of EER volumes ($\mathbf{v}^*_{t-1} = [v^*_{at0}, \forall a]$) and normalized EER inflows ($\mathbf{z}_{t-1}$) from the previous stage are considered state variables.

$$\mathcal{Q}_t(\mathbf{v}^*_{t-1}, \mathbf{z}_{t-1}) = \min \sum_{k\in\mathcal{K}} \sum_{a\in\mathcal{A}} \Bigg[\sum_{g\in\mathcal{G}_a} C^G_{gt} p^G_{gtk} - \sum_{d\in\mathcal{D}_a} C^D_{dt} p^D_{dtk} + C^R r_{atk} \Bigg] + \alpha_t \tag{5a}$$

$$\mathbf{z}_t = \mathbf{\Phi}\mathbf{z}_{t-1} + \boldsymbol{\epsilon}_t \qquad \left(\boldsymbol{\pi}^z\right) \tag{5b}$$

$$I_{at} = \sigma_{at} z_{at} + \mu_{at} \qquad \forall a \tag{5c}$$

$$\mathbf{v}_{t-1} = \mathbf{v}^*_{t-1} \qquad \left(\boldsymbol{\pi}^v\right) \tag{5d}$$

$$v_{atk} - v_{at,k-1} + p^H_{atk} + q^S_{atk} = \zeta_k I_{at} \qquad \forall a,k \tag{5e}$$

$$p^H_{atk} + \sum_{g\in\mathcal{G}_a} p^G_{gtk} - \sum_{d\in\mathcal{D}_a} p^D_{dtk} + r_{atk} + \sum_{\ell\in\mathcal{L}^+_a} f_{\ell tk} - \sum_{\ell\in\mathcal{L}^-_a} f_{\ell tk} \geq D_{atk} - W_{atk} \qquad \forall a,k \tag{5f}$$

$$\alpha_t + \sum_{a\in\mathcal{A}} \pi^v_{act} v_{atK} + \sum_{a\in\mathcal{A}} \pi^z_{act} z_{at} \geq \beta^B_{ct} \qquad \forall c \tag{5g}$$

$$-\overline{F}_{\ell t} \leq f_{\ell tk} \leq \overline{F}_{\ell t} \qquad \forall \ell,k \tag{5h}$$

$$0 \leq p^G_{gtk} \leq \overline{P}^G_{gt} \qquad \forall g,k \tag{5i}$$

$$0 \leq p^D_{dtk} \leq \overline{P}^D_{dt} \qquad \forall g,k \tag{5j}$$

$$\underline{P}^H_{at} \leq p^H_{atk} \leq \overline{P}^H_{at} \qquad \forall a,k \tag{5k}$$

$$\underline{V}_{at} \leq v_{atk} \leq \overline{V}_{at} \qquad \forall a \tag{5l}$$

The objective in (5a) is to minimize the costs associated with operation of the system in the current decision period and the expected cost of operating system in the future. The current cost comes from thermal generation and curtailment of price-inelastic demand, while the coverage of price-elastic demand is seen as a revenue. The future expected cost is represented by α_t which is constrained by Benders cuts in (5g).

A vector autoregressive model of first order representing the weekly normalized inflow to EERs is described in (5b). The correlation matrix ($\mathbf{\Phi}$) and residuals ($\boldsymbol{\epsilon}_t$) are fitted to observations, where residuals are adapted to a three-parameter lognormal distribution according to [39]. The normalized inflow is converted to energy inflow in (5c). Note that the inflow model always generates non-negative energy inflows. In (5d) a copy of the EER reservoir volume state variables are taken, for the ease of finding their dual values $\boldsymbol{\pi}^v$. EER energy balances are provided in (5e). These balances are only considered when feasibility cuts of type (9) are not added to (5), such as in case REF in Section V, to provide a linkage between the initial and final EER storages. An energy balance for each price area and time step is defined in (5f), allowing exchange of energy between price areas. Benders cuts in (5g) are constructed in the backward iteration of the SDDP algorithm based on sensitivities of the state variables, found as dual values from (5b) and (5d), as will be described in Section IV-A. Variable boundaries are presented in (5h)-(5l), where boundaries in (5k) and (5l) are obtained from (4e)-(4f) and (4c)-(4d), respectively.

The decision problem in (5) decides on the EER hydropower generation per time step (p^{H*}_{atk}) and its final stored energy ($\mathbf{v}^*_t = [v^*_{atK}, \forall a]$). These decisions are in turn checked in (6), and feasibility cuts of type (9) may be added to (5) to further constraint the EER decision, as will be elaborated on in the following. Note that additional EER constraints explicitly formulated in (5) could help guiding the decision problem towards feasible EER decisions when no or few feasibility cuts are available, but such experiments were not pursued in this work.

C. Disaggregation

The aggregated hydropower description will tend to overestimate the capability of the detailed hydropower system. In this section it is described how the feasibility of the EER decisions from (5) related to hydropower generation (p^{H*}_{atk}) and energy volume at the end of the decision period ($\mathbf{v}^*_t$) for a state defined by $\mathbf{v}^*_{t-1}$ and I_{at} can be validated considering detailed hydropower description per EER. The EER solution is disaggregated to a detailed representation by applying the same conversion factors and mappings that were used for the aggregation. In the LP problem in (6) the feasibility of the aggregated results is checked.

$$Z_{at}(p^{H*}_{atk}, \mathbf{v}^*_t, \mathbf{v}^*_{t-1}, I_{at}) = \min \sum_{k\in\mathcal{K}} y^P_{kt} + y^E_t \tag{6a}$$

$$v_{htk} + \Gamma_w\Big(q^D_{htk} + q^B_{htk} + q^S_{htk}\Big) - \Gamma_w\Big(\sum_{j\in\omega^D_h} q^D_{jtk} + \sum_{j\in\omega^B_h} q^B_{jtk} + \sum_{j\in\omega^S_h} q^S_{jtk}\Big) = \zeta^V_{aht} v_{a,t-1} + \zeta_k \zeta^I_{aht} I_{at} \qquad \forall h\in\mathcal{H}_a, k=1 \tag{6b}$$

$$v_{htk} - v_{ht,k-1} + \Gamma_w\Big(q^D_{htk} + q^B_{htk} + q^S_{htk}\Big) - \Gamma_w\Big(\sum_{j\in\omega^D_h} q^D_{jtk} + \sum_{j\in\omega^B_h} q^B_{jtk} + \sum_{j\in\omega^S_h} q^S_{jtk}\Big) = \zeta_k \zeta^I_{aht} I_{at} \qquad \forall h\in\mathcal{H}_a, k\in\mathcal{K}\setminus 1 \tag{6c}$$

$$q^D_{htk} = \sum_{n\in\mathcal{N}_h} q^D_{nhtk} \qquad \forall h\in\mathcal{H}_a, k \tag{6d}$$

$$-\Delta_{ht} \leq q^D_{htk} - q^D_{ht,k-1} \leq \Delta_{ht} \quad \forall h\in\mathcal{H}_a, k\in\mathcal{K}\setminus 1 \tag{6e}$$

$$0 \leq q^D_{nhtk} \leq \overline{Q}^D_{nht} \qquad \forall n,h\in\mathcal{H}_a,k \tag{6f}$$

$$0 \leq q^B_{htk} \leq \overline{Q}^B_{ht} \qquad \forall h\in\mathcal{H}_a,k \tag{6g}$$

$$\underline{V}_{ht} \leq v_{htk} \leq \overline{V}_{ht} \qquad \forall h\in\mathcal{H}_a,k \tag{6h}$$

$$\sum_{h\in\mathcal{H}_a}\sum_{n\in\mathcal{N}_h} \Gamma_e \eta_{nh} q^D_{nhtk} + y^P_{kt} \geq p^{H*}_{atk} \quad \left(\gamma^p_{atk}\right) \qquad \forall k \tag{6i}$$

$$\sum_{h\in\mathcal{H}_a} \Gamma_e \eta^{bS}_h v_{hK} + y^E_t \geq v^*_{at} \qquad \left(\gamma^v_{at}\right) \tag{6j}$$

$$v_{a,t-1} = v^*_{a,t-1} \qquad \left(\kappa^v_{at}\right) \tag{6k}$$

$$I_{at} = I^*_{at} \qquad \left(\kappa^i_{at}\right) \tag{6l}$$

The objective in (6a) is to minimize the use of slack variables for constraints (6i) and (6j). Hydropower modules h are connected through the three possible waterways discharge, bypass and spillage. Each module has associated sets comprising upstream modules discharging (ω^D_h), bypassing (ω^B_h) and spilling (ω^S_h) to it. Water balances are defined for the first (6b) and subsequent (6c) time steps for each module, accounting for the hydrological topology provided by the waterways. A concave relationship between power and discharge is facilitated by discharge segments, as described in Section III-A and illustrated in Fig. 2. The total discharge is found in (6d).

This is the accepted version of an article published in IEEE Transactions of Sustainable Energy
https://doi.org/10.1109/TSTE.2022.3214497

Ramping constraints on discharge are included in (6e). Boundaries on discharge, bypass, and reservoir volume are provided in (6f), (6g) and (6h), respectively. These boundaries are often subject to seasonal variations, e.g., due to environmental constraints on river flows and reservoir levels. The constraints in (6i) and (6j) serve to check the feasibility of the schedules of generation per time step and volume at the end of the decision stage obtained from the EER in (5). Finally, copies of the state variables are introduced in (6k) and (6l) to ease the computation of their dual values, which are needed in the creation of feasibility cuts.

Note that the hydropower production function illustrated in Fig. 2 and represented in (6i) can be improved to include the dependency of power output on net head (or reservoir volumes). Improvements need to comply with the convexity of (6) to avoid compromising the validity of the feasibility cuts. As an example, the piecewise linear formulation in [43] which represents the relationship between power production, discharge, volume, and spillage, could be embedded in (6).

The parameters ζ^V_{aht} define the fraction of initial energy reservoir volume to be distributed to the individual reservoirs. In this work ζ^V_{aht} are defined by the relative energy storage capability of the reservoir capacities according to (7a). Similarly, the parameters ζ^I_{aht} defined in (7b) provide fractions of energy inflow volumes to be distributed to the individual reservoirs, and are based on average annual inflow ($\tilde{I}_h$).

$$\zeta^V_{aht} = \frac{\eta^{bS}_h \overline{V}_{ht}}{\sum_{i \in \mathcal{H}_a} \eta^{bS}_i \overline{V}_{it}} \tag{7a}$$

$$\zeta^I_{aht} = \frac{\eta^{bS}_h \tilde{I}_{ht}}{\sum_{i \in \mathcal{H}_a} \eta^{bS}_i \tilde{I}_{it}} \tag{7b}$$

One should strive to let the parameters ζ^V_{ahtk} and ζ^I_{aht} reflect the most likely distribution for each decision stage in the planning horizon. In the case of disaggregating EER storage to hydropower modules, more advanced distribution parameters could resemble different strategies in the typical filling and depletion seasons of the individual reservoirs [30]. The same reasoning cannot be used for inflow, as its disaggregation is determined by nature and not strategic decisions.

Note that the distribution parameters suggested in (7a) and (7b) can be seen as rough estimates, and that higher precision can be introduced by deploying detailed knowledge about the system at hand and its initial state. Although there are different ways of defining the distribution parameters, one should keep in mind that they must be independent of the EER state variables to comply with SDDP convexity requirements and to facilitate cut sharing.

D. Feasibility Cuts

By considering the decision problem in (5) as the master problem and the hydropower feasibility problems in (6) as subproblems, one can apply two-stage Benders decomposition to coordinate the solutions to achieve optimality of (5) while respecting the feasibility check. Let p^{H*}_{atk} and v^*_{at} be a decision from (5) to be evaluated in (6). If this trial decision is feasible, no slack variables are used in (6) and the objective function value Z^*_{at} and dual values in (6) are zero. If not, the linear inequality in (8) (reformulated to (9)) can be constructed and added to (5) to constrain the EER decisions. This inequality involves all subproblem state variables (p^H_{atk}, v_{at}, $v_{a,t-1}$, and I_{at}), and allows EER decision variables (p^H_{atk} and v_{at}) to adjust to prepare for feasible hydropower operation. We use the term *feasibility cut* to describe (9) due to the feasibility check performed in (6) and in line with the terminology and formulation in [40] (Section 5.1.b).

$$\begin{aligned} 0 \geq Z^*_{at} + \sum_{k \in \mathcal{K}} \gamma^p_{atk} \Big(p^H_{atk} - p^{H*}_{atk} \Big) + \gamma^v_{at} \Big(v_{at} - v^*_{at} \Big) \\ + \kappa^v_{at} \Big(v_{a,t-1} - v^*_{a,t-1} \Big) + \kappa^i_{at} \Big(I_{at} - I^*_{at} \Big) \end{aligned} \tag{8}$$

The inequality in (8) can be rearranged as

$$\sum_{k \in \mathcal{K}} \gamma^p_{atk} p^H_{atk} + \gamma^v_{at} v_{at} + \kappa^v_{at} v_{a,t-1} + \kappa^i_{at} I_{at} \leq \beta^F_{at}, \tag{9}$$

where

$$\beta^F_{at} = -Z^*_{at} + \sum_{k \in \mathcal{K}} \gamma^p_{atk} p^{H*}_{atk} + \gamma^v_{at} v^*_{at} + \kappa^v_{at} v^*_{a,t-1} + \kappa^i_a I^*_{at}.$$

The feasibility cut in (9) constrains the solution space for the EER production and storage decisions, and can be added to (5). As the problem formulated in (6) is convex and the SDDP state variables are accounted for, the feasibility cuts in (9) can be shared among different states in the same decision stage [44]. The addition of feasibility cuts (9) to the decision problem (5) do not require additional slack variables to ensure relatively complete recourse in the SDDP algorithm.

Note that the spatial decomposition provided by coordinating solutions of (5) and (6) by feasibility cuts (9) has similarities to Lagrangian Relaxation techniques frequently proposed in the literature for solving the hydrothermal scheduling problem [41]. However, it is not necessary to solve (6) for each time (5) is solved within the SDDP algorithm. In Section IV it is described how the EER feasibility can be constrained by feasibility cuts constructed dynamically as part of the SDDP algorithm or even constructed prior to running SDDP. Although the use of feasibility cuts is well known within multi-stage Benders decomposition algorithms [40], the application to facilitate spatial decomposition within the LTS problem has, to the best of our knowledge, not been addressed in the previous technical literature.

The feasibility cut coefficients are obtained as dual variables from (6i)-(6l). While the coefficients γ^p reflect the marginal cost of the generation requirement in (6i), the coefficients γ^v, κ^v and κ^i reflect the cost (resp. benefit) of having more (resp. less) water available for generation. Provided an initial reservoir volume $v_{a,t-1}$, inflow I_{at} and distribution parameters ζ^V and ζ^I, the constraint in (9) will inform the decision problem in (5) if the proposed:

a) Generation schedule p^{H*}_{atk} is not feasible for all time steps k. In this case (6i) is binding for the non-feasible time steps k' with $\gamma^p_{atk'} = 1.0$, while the other coefficients are zero.
b) Target reservoir volume v^*_{at} is not feasible. In this case (6j) is binding with $\gamma^v_{at} = 1.0$, while the other coefficients are zero.
c) Combination of generation schedule and target volume is not feasible. In this case one or more $0 < \gamma^p_{atk} \leq 1.0$ and $0 < \gamma^v_a \leq 1.0$.

While cases a) and b) concern the capacity of the system, case c) concerns the trade-off between energy generation and energy storage. The different types of cuts are visualized in two dimensions in Fig. 3. The feasible region is colored grey and is constrained by cuts c_1-c_4, where c_1 is of type a), c_2 of type b), and c_3-c_4 of type c).

A cut reflecting case c) informs the optimization problem in (5) that it cannot decide on a high generation and a high final storage at the same time, it needs to compromise on one (or both) of them. Consider the case where (5) suggest maximum generation throughout the decision period. When evaluated in (6), all discharge segments in (6i) are activated, where the last segment has the lowest water conversion efficiency (as illustrated in Fig. 2). Thus, the energy discharge in (5) is likely to underestimate the actual water usage needed in (6) to meet the suggested generation target. Recall, that

This is the accepted version of an article published in IEEE Transactions of Sustainable Energy
https://doi.org/10.1109/TSTE.2022.3214497

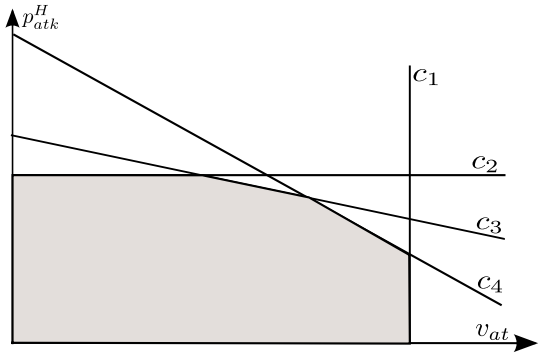

Fig. 3: Feasibility cuts illustrated.

(5) is not explicitly informed about the water to power conversion used in (6i). However, as feasibility cuts are added, this information is implicitly embedded.

IV. Solution Strategy

A main iteration in the SDDP algorithm consists of a forward and a backward iteration as briefly described in Section IV-A. Two different approaches for embedding feasibility cuts in SDDP are then described in Sections IV-B and IV-C.

A. SDDP

1) Forward Iteration: In the SDDP forward iteration a sequence of inflow scenarios $s = 1, \ldots, NS$ covering the period of analysis from $t = 1, \ldots, T$ are defined by randomly sampling residuals from the fitted three-parameter lognormal distribution according to [39] and by use of (5b). Subsequently, the stage decision problem (5) with hydropower EERs is solved for each stage t along the simulated scenario s, and results are collected and state variables are updated for the next stage. The simulated state at the end of the stage is used as the initial state for the next stage. The forward simulation provides an updated set of state trajectories. Moreover, the forward simulation is used to obtain a lower bound J^- in (10) representing the first stage cost plus the future expected cost seen from the first stage, and an upper bound J^+ in (11) representing the average simulated cost.

$$J^- = f_1(x_1, y_1) + \alpha_1 \tag{10}$$

$$J^+ = \frac{1}{NS} \sum_{s=1}^{NS} \sum_{t=1}^{T} f_t(x_{st}, y_{st}) \tag{11}$$

Uncertainty around the upper bound can be used as a convergence check [12]. One computes the standard deviation sd as in (12) and checks if the lower bound (J^-) lies in the interval $\left[J^+ - 1.96\frac{sd}{\sqrt{NS}}; J^+ + 1.96\frac{sd}{\sqrt{NS}}\right]$.

$$sd^2 = \frac{1}{NS-1} \sum_{s=1}^{NS} \Big(\sum_{t=1}^{T} f_t(x_{st}, y_{st}) - J^+ \Big)^2 \tag{12}$$

As discussed in the literature, e.g. in [24] and [45], this statistical convergence criterion has limitations, and for practical purposes the stabilization of the lower bound may serve as an alternative criterion [45].

2) Backward Iteration: Benders cuts at the end of the planning horizon $t = T$ can be obtained from a predefined final value function Ψ. For $t = T-1, \ldots, 1$ in the backward iteration one loops through each state trajectory obtained from the last forward iteration. Starting from the state at the end of stage $t-1$, for each realization of stochastic variables one computes the optimal operation for stage t by solving (5). From the sensitivities of the objective function to the initial state values, found as dual values from (5b) and (5e), new Benders cuts of type (5g) at the end of stage $t-1$ are obtained.

B. Dynamic Feasibility Cuts

In principle, the feasibility check per EER defined in (6) can be carried out for each solved instance of (5) in both the forward and backward iterations of the SDDP algorithm. Feasibility cuts of type (9) are then built dynamically for each stage and EER and added to the set of cuts $\mathcal{C}^F_{at}$. For a given state and decision stage, the following steps are carried out:

1. Solve (5) with existing feasibility cuts (9) in $\mathcal{C}^F_{at}, \forall a \in \mathcal{A}$.
2. Check if the trial solutions p^{H*}_{atk} and v^*_{at} are feasible by solving (6) for all EERs.
3. If not, add a new feasibility cut of type (9) to $\mathcal{C}^F_{at}$ for EERs with infeasible trial solutions.

To limit the computational expense involved with solving (6), it was found efficient checking hydropower feasibility only in the forward SDDP iteration. That is, step 1 is carried out in both the forward and backward SDDP iterations, while steps 2 and 3 are only carried out in the forward iterations.

C. Static Feasibility Cuts

The detailed hydropower problem in (6) depends on the SDDP state variables for the particular EER, but does not explicitly depend on the SDDP strategies represented by Benders cuts in (5g). Thus, it is possible to evaluate (6) prior to an SDDP run for a selection of state variables. The following steps were conducted to create feasibility cuts a priori.

1. Sample a large number of inflow scenarios I_{at}, for $t = 1, \ldots, T$ from (5b) and (5c).
2. Represent $v_{a,t-1}$ as a set of points covering the interval $[\underline{V}_{at}, \overline{V}_{at}]$. For each value of $v_{a,t-1}$, define a range of feasible volumes $[\underline{V}^*_{at}, \overline{V}^*_{at}]$ for the end of stage t.
3. Sample hydropower generations p^{H*}_{atk} between $[\underline{P}^H_{at}, \overline{P}^H_{at}]$ and energy reservoir volumes v^*_{at} between $[\underline{V}^*_{at}, \overline{V}^*_{at}]$.
4. For each EER, check if the samples p^{H*}_{atk} and v^*_{at} are feasible for the corresponding state variables $v_{a,t-1}$ and I_{at} by solving (6).
5. If not, create a new cut c of type (9).
6. Check if cut c is equal to existing cuts in $\mathcal{C}^F_{at}$. If not, add c to $\mathcal{C}^F_{at}$.

A large number of feasibility cuts can be generated prior to the SDDP run with the above procedure. Since the solution of (6) is part of a two-stage decomposition process and does not depend on the SDDP strategies, the feasibility cuts are tight. However, as the share of equal cuts may be substantial, the equality check in step 6 above serves an important role in limiting the size of $\mathcal{C}^F_{at}$.

V. Computational Experiments

A. System and Case Description

An LTS model based on SDDP applied to the aggregated hydropower description and with feasibility cuts was implemented in `Julia`, using the `JuMP` package [46]. Computational tests were carried out on a test system comprising 4 price areas, with a combination of generation technologies and grid topology as indicated in Fig. 4. Approximately 70 % of the installed generation capacity in the test system is from hydropower, the rest is covered by a mix of wind and thermal power. A total of 20 thermal units with variable marginal costs are represented.

This is the accepted version of an article published in IEEE Transactions of Sustainable Energy
https://doi.org/10.1109/TSTE.2022.3214497

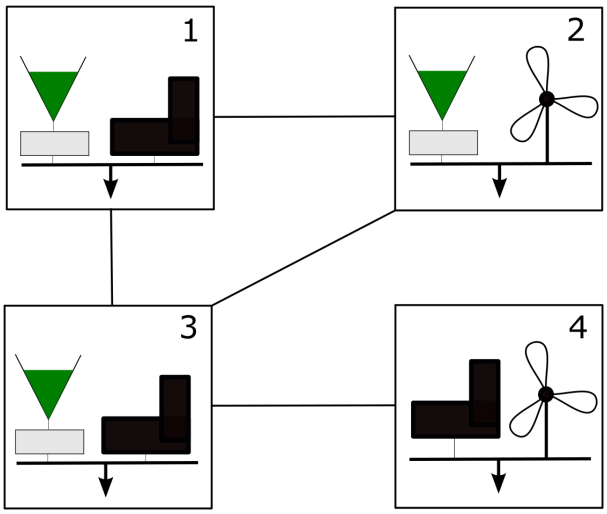

Fig. 4: Test system topology and mix of generation technologies (hydro, wind, and thermal power).

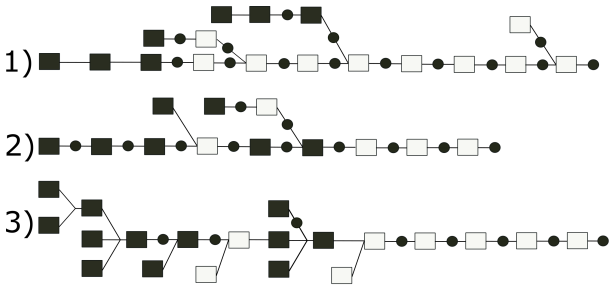

Fig. 5: Topologies for hydropower watercourses in areas 1-3. Upstream reservoirs are to the left.

Price areas 1-3 each comprise a hydropower watercourse, as illustrated in Fig. 5, representing real hydropower systems located in Norway. Reservoirs in Fig. 5 are shown as rectangles, where the color black indicates a reservoir with non-zero storage capacity, while white indicates reservoirs without storage capacity, i.e., run-of-river plants. Black circles indicate hydropower plants. All reservoirs receive inflow. The 33 power stations have different numbers of discharge segments, in the range 1-7, to represent their production functions, as illustrated in Fig. 2.

All tests were carried out on an Intel Core i7-9850H processor with maximum frequency of 4.60 GHz and 64 GB RAM. CPLEX version 12.10 was used to solve the LP problems, using the dual Simplex algorithm. Parallel processing of the SDDP algorithm was not applied.

A scheduling horizon of 3 years was applied with weekly decision stages. Each week was divided into 56 time steps each with a length of 3 hours. Ramping constraints on discharge were considered only for the results presented in Section V-E. A total of 200 inflow scenarios were re-sampled in each forward SDDP iteration, and 12 discrete inflow white noise terms were sampled at each stage in the backward SDDP iterations. Consequently, a total of $200 \times 156 = 31200$ decision problems of type (5) are solved in the forward iteration and $200 \times 12 \times 156 = 374400$ in the backward iteration. The stabilization of the lower bound obtained from (10) indicates that further iterations of the SDDP algorithm do not significantly improve the constructed policy and can be used as a practical convergence criterion [45]. A maximum number of 100 iterations was applied in the experiments, which turned out to be stricter than the statistical convergence criterion described in Section IV-A1.

Four separate cases were considered:

1. *Reference* (REF) using the SDDP formulation described in Section IV-A, with weekly decision problems in (5), and without feasibility cuts.
2. *Dynamic Feasibility Cuts* (DYN-FC) using the same SDDP formulation as in REF, but with dynamic construction and addition of feasibility cuts (9) in the forward SDDP iterations, as described in Section IV-B.
3. *Static Feasibility Cuts* (STAT-FC) using the same SDDP formulation as in REF, but with pre-computed feasibility cuts (9) as described in Section IV-C.
4. *Detailed Formulation* (DET) using the same SDDP formulation as in REF, but with explicit inclusion of detailed the hydropower representation (6) in the decision problem in (5). Problem (6) is coupled with (5) by treating EER decisions p^H_{atk} and v_{at} as variables instead of parameters in (6i) and (6j), respectively.

Note that (5e) was included in case REF, but excluded in cases DYN-FC, STAT-FC and DET, for reasons discussed in Section III-B.

For case DYN-FC, a maximum of 200 new feasibility cuts are built in each forward iteration for each stage. These cuts will accumulate with the forward iterations. In case STAT-FC we initially created 100000 cuts per stage according to the description in Section IV-C. By removing equal cuts, the number of feasibility cuts to be considered per stage of the SDDP run was in the range of 500-1000. For all cases, Benders cuts of type (5g) were constructed and added iteratively in the SDDP backward iteration as described in IV-A, and accumulated without further cut management.

B. Single Scenario

To test the convergence properties of the model, it was run for a pre-sampled single scenario, i.e., with deterministic inflow in both the forward and backward iterations of the SDDP algorithm. Fig. 6 shows how the cost bounds converge for cases DYN-FC, STAT-FC and DET. The three cases converge to a cost gap of 0.001 k€ within 65 (DET), 67 (STAT-FC) and 109 (DYN-FC) iterations. Case REF converges in 53 iterations to a cost that is approximately 5% lower than for the other cases, and is therefore not shown in this figure. The DET and DYN-FC cases converge at the same objective value, while STAT-FC converges at a value that is approximately 30 k€ lower. The lower objective value can be explained by the fact that not all states can possibly be covered by the sampling in the cut creation procedure applied in STAT-FC.

A single feasibility cut is built in each forward iteration for each stage in DYN-FC, leading to a rather slow convergence process shown in Fig. 6. On the other DYN-FC is significantly faster. The total computation times were 38 sec (DYN-FC), 213 sec (STAT-FC) and 1250 sec (DET). This demonstrates that DYN-FC is efficient in creating feasibility cuts along a single scenario, while STAT-FC create these cuts without knowledge about the hydropower generation and reservoir trajectory. Explicit formulation of the detailed hydropower in case DET is significantly slower than using feasibility cuts. This can be explained by the size of the LP problems solved. While the LP problem of type (5) including feasibility cuts (9) for STAT-FC on average comprises 2.5k variables and 1.8k constraints, the DET LP problems where (5) and (6) are combined comprises 19k variables and 12k constraints.

C. Computational Performance

The convergence characteristic of the algorithm is shown in Fig. 7, comparing the lower bounds for all cases for the first 50 iterations.

This is the accepted version of an article published in IEEE Transactions of Sustainable Energy
https://doi.org/10.1109/TSTE.2022.3214497

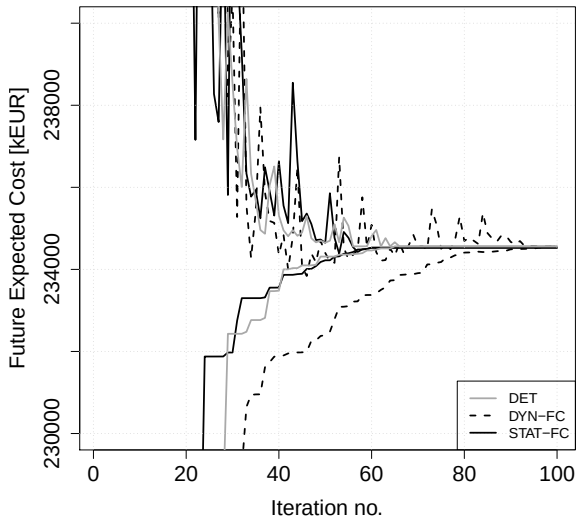

Fig. 6: Convergence characteristics for a single scenario. Upper and lower bounds for cases DYN-FC, STAT-FC and DET.

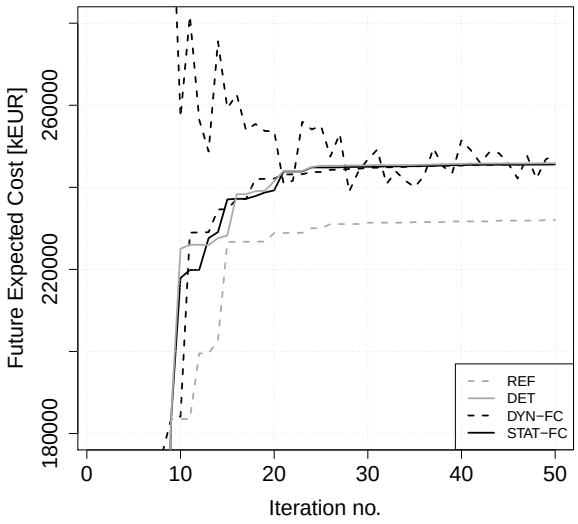

Fig. 7: Convergence characteristics. Lower bounds for all cases and upper bound for case DYN-FC.

The upper bound for case DYN-FC is included to show how the gap between the upper and lower bound gradually decreases with iterations. Stable lower bounds were observed for all cases within the maximum number of iterations. Both DYN-FC and STAT-FC converge to approximately the same lower cost bound, which is 5.9 % higher than the REF bound. Clearly, the feasibility cuts have constrained the operation of the hydropower EERs, leading to a higher expected cost of operating the system over the scheduling horizon. The lower bound of case DET is approximately 110 k€ (or 0.045 %) higher than that of DYN-FC and STAT-FC after 100 iterations. Comparing the DYN-FC lower bound in the deterministic case (Fig. 6) and stochastic (Fig. 7) shows that the convergence rate is significantly improved in the latter case when up to 200 new feasibility cuts are constructed per forward iteration.

The computation times for all cases are shown in Table I, measured as time spent per iteration for the first, middle and last iteration, as well as the total time. Since all cases accumulate Benders cuts of type (5g), an increase in computation time per iteration was expected. The REF case does not consider feasibility cuts and is therefore faster to solve than DYN-FC and STAT-FC. Comparing DYN-FC and STAT-FC, the former is considerably faster in the first iteration, but gradually slows down with iterations as the number of feasibility cuts grows. On the other hand, STAT-FC considers a fixed number of feasibility cuts and has a comparatively modest increase in computation time from iteration 1 to 100. No direct comparison with a SDDP model for the detailed system without aggregation was made in this work. However, the significant increase in computation time for case DET, which represents the detailed hydropower explicitly, demonstrates the computational efficiency of cases DYN-FC and STAT-FC. It should be noted that there is considerable potential to further speed up the computation time by use of cut management techniques (such as relaxation or declaration of lazy constraints), since only a few feasibility cuts are binding at the time.

TABLE I: Computation times, in seconds.

Case	Iter no. 1	Iter no. 50	Iter no. 100	Total
REF	3.2	5.1	11.4	370
DYN-FC	4.1	294.0	736.5	14347
STAT-FC	39.9	52.8	77.5	3204
DET	158.0	1346.0	11941.0	229130

D. Simulation Results

To compare the simulated results for the different cases, 2000 inflow scenarios were sampled and operation along these were simulated with the strategies and feasibility cuts obtained from all cases. Since differences in simulation results between the DYN-FC and STAT-FC cases are muted, only REF and STAT-FC results are compared in the following.

Fig. 8 presents the duration curves for simulated EER generation for area 2. It can be observed that the total amount of generation for the two cases are similar, which is reasonable since the energy inflow is the same in both cases. Furthermore, the maximum and minimum generation levels are less exploited in the constrained STAT-FC case. This can be explained by the tendency of case REF to overestimate EER generation capability, due to optimistic information about generation efficiency and stored energy.

Fig. 9 shows the weekly average power prices for area 3 obtained from REF and STAT-FC, as the mean, 0 and 100 percentiles. These prices were obtained as the dual values from (5f). The limited flexibility of hydropower in case STAT-FC contributes to increased price levels on average as well as higher price spikes.

E. Ramping Constraints

Case STAT-FC was run for different levels of maximum allowed ramping on discharge, by setting Δ_h in (6e) equal to a certain percentage of the maximum discharge capacity for a set of relevant modules. For each ramping level, SDDP was run separately according to the setup defined in Section V-A, followed by a simulation considering the same 2000 sampled inflow scenarios as used in Section V-D. The "activation" of (6e) is explicitly seen in the evaluation of the detailed hydropower system, and communicated to the SDDP decision problem through feasibility cuts. Table II shows the expected simulated costs for the different levels of maximum allowed ramping on discharge considered. The last line in Table II shows how the expected cost of operating the system increases (in percentage) with decreasing maximum ramping capacity on discharge.

This is the accepted version of an article published in IEEE Transactions of Sustainable Energy
https://doi.org/10.1109/TSTE.2022.3214497

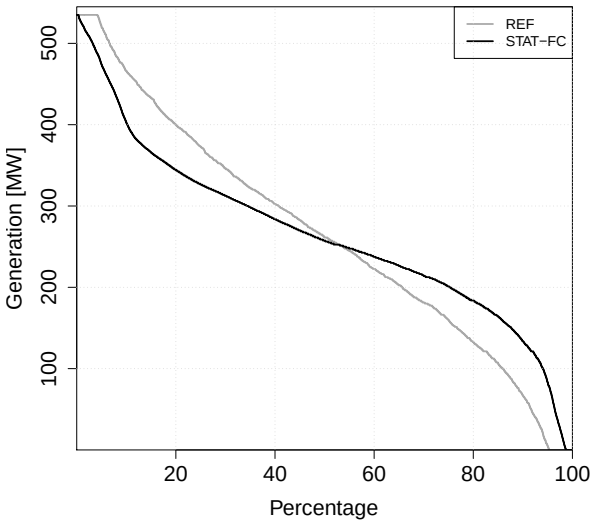

Fig. 8: Duration curves for generation from EER in area 2.

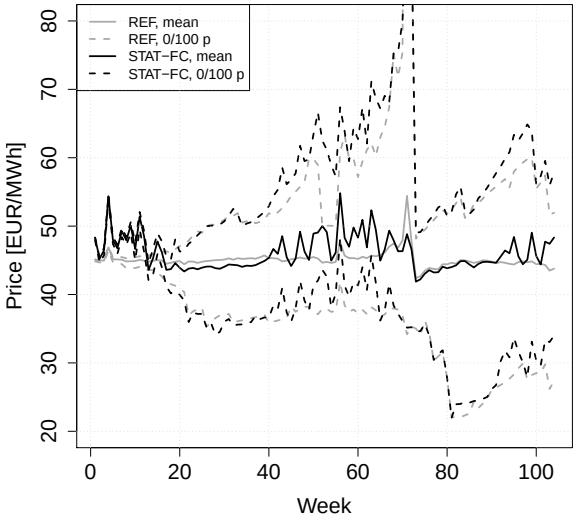

Fig. 9: Weekly average power prices for area 3.

Fig. 10 shows the duration curves for generation for the EER in price area 3 for different levels of maximum allowed ramping. As ramping capability is gradually limited, generation close to the maximum and minimum boundaries becomes less frequent, and the duration curve takes a flatter profile. This illustrates how the flexibility of the hydropower is limited with stricter ramping constraints.

VI. Conclusions

This work considers an SDDP model representing the aggregated hydropower as a reference and presents a method for facilitating the interaction between aggregated and detailed hydropower by applying spatial decomposition principles. Feasibility cuts obtained by optimizing the detailed hydropower system are used to constrain the flexibility of the aggregated hydropower system. The construction and use of feasibility cuts fits well into the SDDP algorithm and can even be computed prior to an SDDP run. The method was demonstrated on a test system comprising three realistic and rather complex hydropower watercourses.

TABLE II: Impact of ramping constraints on discharge.

Max. ramp.	100%	80%	50%	30%
Exp. cost [k€]	245694	245977	248383	256007
Increase (%)	0.00	0.12	1.09	4.20

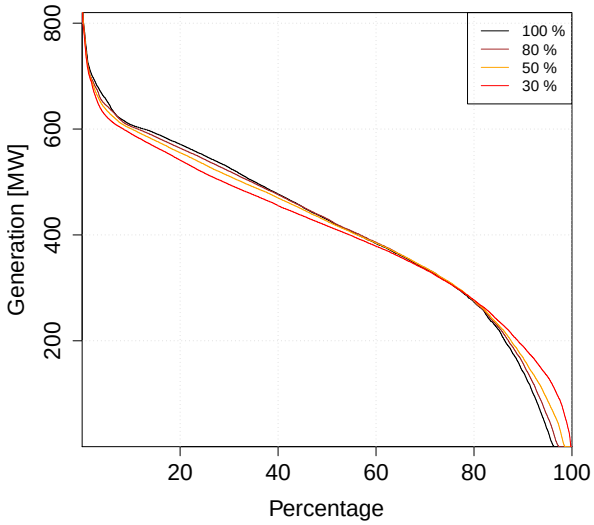

Fig. 10: Duration curves for generation from EER in price area 3 considering different levels of maximum ramping on discharge.

The test results show that the inclusion of feasibility cuts significantly increases computation time. However, the low dimensionality in terms of aggregated reservoir volumes and inflows is maintained, and SDDP convergence rates do not change notably. Computing feasibility cuts prior to an SDDP run proved to be faster than cut creation within SDDP. It was demonstrated that implicit representation of detailed hydropower through feasibility cuts served to constrain the flexibility of the aggregated hydropower system. Moreover, the tests demonstrated how changes in the detailed system, exemplified by the addition of maximum discharge ramping constraints, are naturally captured by the proposed method.

When evaluating the proposed method against the reference case that does not consider feasibility cuts, the trade-off between increased precision in results versus increased computation time is central. The increased result precision is clearly demonstrated in the case studies, but one could argue that the EER applied in the reference case could be further constrained by adjusting the EER parameters. On the other hand, the estimated increase in computation time when using feasibility cuts is not discouraging compared to an explicit formulation of the detailed hydropower system.

Promising avenues for further research involve testing on large-scale systems, improved management of feasibility cuts, inclusion of more hydropower details (such as head dependencies), and improved factors for distribution of reservoir and inflow energy to the detailed system.

References

[1] J. I. Pérez-Díaz, M. Belsnes, and A. L. Diniz, “Optimization of Hydropower Operation,” *Comprehensive Renewable Energy*, vol. 6, pp. 84–104, 2022.

This is the accepted version of an article published in IEEE Transactions of Sustainable Energy
https://doi.org/10.1109/TSTE.2022.3214497

[2] A. Helseth and A. C. G. Melo, "Scheduling Toolchains in Hydro-Dominated Systems," SINTEF Energy Research, techreport 2020-000757, 2020.

[3] Z. G. A. Philpott, "Models for estimating the performance of electricity markets with hydro-electric reservoir storage," Electric Power Optimization Centre, University of Auckland, New Zealand, Tech. Rep., 2013.

[4] S. Jaehnert, O. Wolfgang, H. Farahmand, S. Völler, and D. Huertas-Hernando, "Transmission expansion planning in Northern Europe in 2030—Methodology and analyses," *Energy Policy*, vol. 61, pp. 125–139, 2013.

[5] R. M. Chabar, S. Granville, M. V. F. Pereira, and N. A. Iliadis, *Optimization of Fuel Contract Management and Maintenance Scheduling for Thermal Plants in Hydro-based Power Systems*, ser. Energy, Natural Resources and Environmental Economics. Springer, Berlin, Heidelberg, 2010, ch. 13, pp. 201–219.

[6] T. N. Santos, A. L. Diniz, C. H. Saboia, R. N. Cabral, and L. F. Cerqueira, "Hourly Pricing and Day-Ahead Dispatch Setting in Brazil: The DESSEM Model," *Electric Power Systems Research*, vol. 189, no. 106709, 2020.

[7] J. Kong, H. I. Skjelbred, and O. B. Fosso, "An overview on formulations and optimization methods for the unit-based short-term hydro scheduling problem," *Electric Power Systems Research*, vol. 178, 2020.

[8] A. Brigatto, A. Street, and D. M. Valladão, "Assessing the cost of time-inconsistent operation policies in hydrothermal power systems," *IEEE Transactions on Power Systems*, vol. 32, no. 6, pp. 4914–4923, 2017.

[9] L. Bernardinelli and L. S. A. Martins, "Equilibrium approach to the single solution of longer- and shorter-term hydro-thermal scheduling problems," in *6th International Conference on Clean Electrical Power*, Santa Margherita Ligure, Italy, 2017.

[10] J. W. Labadie, "Optimal operation of multireservoir systems: State-of-the-art review," *Journal of Water Resources Planning and Management*, vol. 130, no. 2, pp. 93–111, 2004.

[11] A. R. de Queiroz, "Stochastic hydro-thermal scheduling optimization: An overview," *Renewable and Sustainable Energy Reviews*, vol. 62, pp. 382–395, 2016.

[12] M. V. F. Pereira and L. M. V. G. Pinto, "Multi-stage stochastic optimization applied to energy planning," *Mathematical Programming*, vol. 52, pp. 359–375, 1991.

[13] A. Gjelsvik, B. Mo, and A. Haugstad, *Handbook of Power Systems I*. Springer, 2010, ch. Long- and medium-term operations planning and stochastic modelling in hydro-dominated power systems based on stochastic dual dynamic programming, pp. 33–55.

[14] E. Pereira-Bonvallet, S. Püschel-Løvengreen, M. Matus, and R. Moreno, "Optimizing hydrothermal scheduling with non-convex irrigation constraints," *Energy Procedia*, vol. 87, pp. 132–150, 2016.

[15] M. Maceira, D. Penna, A. Diniz, R. Pinto, A. Melo, C. Vasconcellos, and C. Cruz, "Twenty Years of Application of Stochastic Dual Dynamic Programming in Official and Agent Studies in Brazil – Main Features and Improvements on the NEWAVE Model," in *Proc. 20th Power System Computation Conference*, 2018.

[16] A. Philpott and V. de Matos, "Dynamic sampling algorithms for multi-stage stochastic programs with risk aversion," *European Journal of Operational Research*, vol. 218, no. 2, pp. 470–483, 2012.

[17] A. Shapiro, W. Tekaya, M. P. Soares, and J. Paulo da Costa, "Worst-Case-Expectation Approach to Optimization Under Uncertainty," *Operations Research*, vol. 61, no. 6, pp. 1435–1449, 2013.

[18] S. Rebennack, "Combining sampling-based and scenario-based nested Benders decomposition methods: application to stochastic dual dynamic programming," *Mathematical Programming*, vol. 156, no. 1, pp. 343–389, 2016.

[19] A. Street, A. Brigatto, and D. M. Valladão, "Co-optimization of energy and ancillary services for hydrothermal operation planning under a general security criterion," *IEEE Transactions on Power Systems*, vol. 32, no. 6, pp. 4914–4923, 2017.

[20] J. Zou, S. Ahmed, and X. A. Sun, "Stochastic dual dynamic integer programming," *Mathematical Programming*, vol. 175, no. 1-2, pp. 461–502, 2018.

[21] A. Papavasiliou, Y. Mou, L. Cambier, and D. Scieur, "Application of Stochastic Dual Dynamic Programming to the Real-Time Dispatch of Storage Under Renewable Supply Uncertainty," *IEEE Transactions on Sustainable Energy*, vol. 9, no. 2, pp. 547–558, 2018.

[22] A. Helseth, M. Fodstad, and B. Mo, "Optimal hydropower maintenance scheduling in liberalized markets," *IEEE Transactions on Power Systems*, vol. 33, no. 6, pp. 6989–6998, 2018.

[23] K. S. Gjerden, A. Helseth, B. Mo, and G. Warland, "Hydrothermal scheduling in Norway using stochastic dual dynamic programming; a large-scale case study," in *In proc. of IEEE PowerTech*, Eindhoven, The Netherlands, 2015.

[24] T. Homem-de-Mello, V. L. de Matos, and E. C. Finardi, "Sampling strategies and stopping criteria for stochastic dual dynamic programming: a case study in long-term hydrothermal scheduling," *Energy Systems*, vol. 2, pp. 1–31, 2011.

[25] V. L. de Matos and E. C. Finardi, "A computational study of a stochastic optimization model for long term hydrothermal scheduling," *International Journal of Electrical Power and Energy Systems*, vol. 43, no. 1, pp. 1443–1452, 2012.

[26] N. V. Arvanitidis and J. Rosing, "Composite Representation of a Multireservoir Hydroelectric Power System," *IEEE Transactions on Power Apparatus and Systems*, vol. 89, no. 2, pp. 319–326, 1970.

[27] M. V. F. Pereira and L. M. V. G. Pinto, "Stochastic optimization of a multireservoir hydroelectric system: A decomposition approach," *Water Resources Research*, vol. 21, no. 6, pp. 779–792, 1985.

[28] V. R. Sherkat, R. Campo, K. Moslehi, and E. O. Lo, "Stochastic Long-Term Hydrothermal Optimization for a Multireservoir System," *IEEE Transactions on Power Apparatus and Systems*, vol. 104, no. 8, pp. 2040–2050, 1985.

[29] J. L. Brandao, "Performance of the Equivalent Reservoir ModellingTechnique for Multi-Reservoir Hydropower Systems," *Water Resources Management*, vol. 24, pp. 3101–3114, 2010.

[30] O. J. Botnen, A. Johannesen, A. Haugstad, S. Kroken, and O. Frøystein, "Modelling of hydropower scheduling in a national/international context," in *Hydropower 92*, E. Brock and D. Lysne, Eds., Lillehammer, 1992.

[31] O. Wolfgang, A. Haugstad, B. Mo, A. Gjelsvik, I. Wangensteen, and G. Doorman, "Hydro reservoir handling in Norway before and after deregulation," *Energy*, vol. 34, no. 10, pp. 1642–1651, 2009.

[32] M. E. P. Maceira, V. S. Duarte, D. D. J. Penna, and M. P. Tcheou, "An approach to consider hydraulic coupled systems in the construction of equivalent reservoir model in hydrothermal operation planning," in *Proc. 17th Power Systems Computation Conference (PSCC)*, Stockholm, Sweden, 2011.

[33] V. L. de Matos, E. C. Finardi, and E. L. da Silva, "Comparison between the Energy Equivalent Reservoir per Subsystem and per Cascade in the Long-Term Operational Planning in Brazil," in *Proc. of EngOpt*, 2008.

[34] M. Löschenbrand and M. Korpås, "Hydro Power Reservoir Aggregation via Genetic Algorithms," *Energies*, vol. 10, no. 12, 2017.

[35] E. Shayesteh, M. Amelin, and L. Söder, "Multi-Station Equivalents for Short-Term Hydropower Scheduling," *IEEE Transactions on Power Systems*, vol. 31, no. 6, pp. 4616–4625, 2016.

[36] E. Blom, L. Söder, and D. Risberg, "Performance of multi-scenario equivalent hydropower models," *Electric Power Systems Research*, vol. 187, 2020.

[37] V. Guigues, "SDDP for some interstage dependent risk-averse problems and application to hydro-thermal planning," *Computational Optimization and Applications*, vol. 57, pp. 167–203, 2014.

[38] A. L. Diniz, M. E. P. Maceira, C. L. V. Vasconcellos, and D. D. J. Penna, "A combined SDDP/Benders decomposition approach witha risk-averse surface concept for reservoir operation in long-term power generation planning," *Annals of Operations Research*, vol. 292, pp. 649–681, 2020.

[39] M. E. P. Maceira and C. V. Bezerra, "Stochastic Streamflow Model for Hydroelectric Systems," in *Proc. 5th conf. on Probabilistic Methods Applied to Power Systems*, 1997.

[40] J. R. Birge and F. Louveaux, *Introduction to Stochastic Programming*, 2nd ed. Springer, 2011.

[41] A. Helseth, S. Jaehnert, and A. L. Diniz, "Convex Relaxations of the Short-Term Hydrothermal Scheduling Problem," *IEEE Transactions on Power Systems*, vol. 36, no. 4, pp. 3293–3304, 2021.

[42] V. Guigues and C. Sagastizábal, "The value of rolling-horizon policies for risk-averse hydro-thermal planning," *European Journal of Operational Research*, vol. 217, no. 1, pp. 129–140, 2012.

[43] A. Diniz and M. E. P. Maceira, "A four-dimensional model of hydro generation for the short-term hydrothermal dispatch problem considering head and spillage effects," *IEEE Transactions on Power Systems*, vol. 23, no. 3, pp. 1298 – 1308, 2008.

[44] G. Infanger and D. P. Morton, "Cut sharing for multistage stochastic linear programs with interstage dependency," *Mathematical Programming*, vol. 75, no. 2, pp. 241–256, 1996.

[45] A. Shapiro, "Analysis of stochastic dual dynamic programming method," *European Journal of Operational Research*, vol. 209, no. 1, pp. 63–72, 2011.

[46] I. Dunning, J. Huchette, and M. Lubin, "JuMP: A modeling language for mathematical optimization," *SIAM Review*, vol. 59, no. 2, pp. 295–320, 2017.

This is the accepted version of an article published in IEEE Transactions of Sustainable Energy
https://doi.org/10.1109/TSTE.2022.3214497